Romanian Reports in Physics, Vol. 57, No. 4, P. 845–872, 2005

STIMULATED EMISSION, SOLID-STATE QUANTUM ELECTRONICS AND PHOTONICS: RELATION TO COMPOSITION, STRUCTURE AND SIZE

I. URSU, V. LUPEI

Laboratory of Solid-State Quantum Electronics, National Institute of Laser, Plasma and Radiation Physics Bucharest-Romania

(Received July 22, 2005)

Abstract. The paper discusses the relation of the radiation emission properties of the doped photonic materials with the composition, structure and size of these materials. It is shown that a proper use of this relation can extend or improve the performances of the photon sources and of their applications.

Key words: quantum electronics, stimulated emission, solid state lasers.

1. INTRODUCTION

A problem of major concern for Einstein was the nature and properties of radiation. The first of the major papers published by Einstein in *annus mirabilis* 1905 was "Uber einen die Erzeugung und Verwandlung des Lichtes betreffenden heuristichen Gesichtspunkt" ("On a heuristic point of view about the creation and conversion of light"), Ann. der Physik 17, 132 (1905). This paper, which is frequently referred to as the paper on the photoelectric effect, is a crucial contribution to the knowledge of the properties of radiation. It extends the work of Planck on the emission of energy quanta by showing that the electromagnetic field of light is in itself composed of energy quanta related to the frequency of light, which have been subsequently named photons; these quanta move without being divided and can be absorbed and emitted only as a whole. With this theory he could explain consistently the characteristics of the photoelectric effect, particularly the dependence of the number of released electrons, but not of their energy, on the intensity of the incident light, while the energy of released electrons is, above a given threshold, related to the frequency of the incident light. The importance of this work was recognized by the Nobel prize awarded in 1921. Einstein's interest in the absorption and emission of light continued and culminated with the paper "Zur Quantentheorie der Strahlung" ("On the quantum theory of

radiation") published in Zeitscrift fur Physik 18, 121 (1917). In this work he used the concept of stationary states of the electrons in atoms, introduced a few years earlier by Bohr, to show that the interaction of these systems with the electromagnetic radiation has two major effects, absorption and stimulated emission, characterised by the Einstein coefficients B_{12} and B_{21}, which, together with the spontaneous emission (Einstein coefficient A) characterize completely the flow of excitation. The existence of absorption and spontaneous emission was known and in large use at the time; however, the stimulated emission by which an excited quantum system can interact resonantly with an electromagnetic radiation and emit a radiation identical in all aspects to the incident radiation was conceptually new, although already in 1913 Einstein assumed that such process could take place in stars. The paper of 1917 connected in a unitary theory the rates of all these three processes and their dependence on the radiation frequency and on the conditions of excitation. Einstein's papers had a very strong impact on the bases of the atomic physics and prepared the road towards new areas of science and technique, the quantum electronics, then the photonics.

In a quantum system the balance between the induced processes, *i.e.*, absorption and stimulated emission by interaction with an incident electromagnetic radiation depends on the ratio of the populations of the upper and the lower energy level connected by the energy quantum of radiation. At thermal equilibrium the population of the upper energy states is smaller than that of the lower levels: in the case of levels separated by energies corresponding to the optical spectrum this difference is exceedingly large, so at thermal equilibrium light emitted by stimulated emission will be extremely weak compared to absorption. Moreover, stimulated emission will also compete with the spontaneous emission. Thus it is no wonder that in a context dominated by thermal equilibrium the stimulated emission did not arouse special interest, although its existence was proved experimentally in 1929 by Landenburg and Kopfermann. However, the stimulated emission bears in itself a very important property: it amplifies the incident resonant radiation by adding identical photons. Since in thermal equilibrium the stimulated emission alone is not enough to grant construction of an amplifying device, a special situation in which the populations of the energy levels are modified so as that of the excited level would be dominant (inversion of population), must be created. It is also obvious that in a quantum system with only two energy levels in interaction with a resonant radiation the most that could be obtained is equalization of populations, but not inversion.

The idea of amplification of radiation by stimulated emission in a quantum system with inversion of population was discussed in several papers, but it did not develop markedly till after World War II, when the need for intense monochromatic sources at wavelengths shorter than available from the vacuum tubes that would extend the capabilities of microwave spectroscopy was put forth. This was a

natural extension of the work performed during the war for development of short-wavelength radiation sources in the frame of the project Radar at MIT Radiation Laboratory and Columbia Radiation Laboratory. This circumstance was very fortunate since it joined the expertise of two branches of science, the physics (mainly atomic and quantum physics, spectroscopy and optics) and the electronic engineering. It was then realised that the stimulated emission in quantum systems with excited levels in the microwave range could be used as driving process for such devices. Energy levels with gaps in the microwave range could be met in various quantum systems, such as molecules (vibrational levels), crystals with paramagnetic ions (the electronic Zeeman levels of the ground electronic state) or free atoms. For such systems the difference in thermal population between the emitting and the terminal level is quite small and inversion is not an exceedingly difficult task A very important innovation resulted from this interplay of physicists and electronic engineers was the resonant feedback necessary to grant a high degree of amplification by stimulated emission that generally cannot be achieved by a single pass of radiation inside the quantum system; when the gain granted by the feedback system overcomes the internal and the out-coupling losses a beam of coherent radiation is produced. It became apparent that such amplifying device would consist of three main components: (i) the active medium that contains the quantum system; its characteristics (the amount of active centers, the geometrical shape and so on) are designed to grant proper conditions for inversion of population and amplification; (ii) the pumping system that enables a high degree of population of the excited level involved in the amplifying transition; (iii) the resonator, that grants a proper feedback of the amplified beam inside the active medium and emission of large number of quanta in single modes. Such devices proved successful in 1954 for generation in the centimetre range by using as active medium a beam of ammonia molecules in excited state separated by electrostatic deviation. In 1957 the concept of three-level-scheme was proposed, in which the act of absorption is decoupled from stimulated emission; very soon emission in centimetre range based on this scheme was demonstrated in paramagnetic solid-state materials such as gadolinium ethyl sulphate or diluted ruby crystals; in these devices the pumping was accomplished by paramagnetic resonance absorption in an energy level placed above the emitting level. This device was named MASER, the acronym for Microwave Amplification by Stimulated Emission of Radiation. While work for development or improvement of masers continued, the extension of the wavelength range did not envisage the millimetre or sub-millimetre radiation, but directly the optical range. It is worth to mention that whereas the invention of the maser responded to a definite practical need, the extension to the optical range was essentially fundamental research aimed to extending the basic knowledge on the interaction of quantum systems with electromagnetic field at optical frequencies. On other hand, this extension was not straightforward, having in view the essential differences between the quantum systems and the energy quantum scale involved

in these devices. The theory of such "Optical Maser" was developed in the 1958 paper of Schawlow and Towness where the main conditions for realization of such devices are discussed. Construction of the optical masers introduced new problems; it was found that for many of these problems basic solution already existed at least at the level necessary for demonstration. Thus, while in case of masers construction of a resonator of the size of wavelength did not put any problem, in case of the optical masers such thing would not be possible. This was circumvented by the use of an open resonator and it was realized that a simple Fabri-Perot resonator consisting of two parallel mirrors, one with total reflection, the other with a small transmission at the wavelength of emission, could act as resonator and provide a very good feedback and selection of modes and extraction of a highly directional coherent beam. An active medium in shape of a cylinder with flat ends was recommended. It was also found that the inversion of population could be achieved by the optical pumping proposed earlier by A. Kastler. The paper discussed the possibility of using as active materials metal vapours, such as potassium, or crystals doped with ions from the transitional groups with energy level schemes favourable to optical pumping and to emission in the optical range (visible and near infrared). Further papers argued that the three-level emission schemes are not the most favourable, especially in case of quantum systems with low quantum efficiency and low emission cross-sections, due to the difficulties to create the population inversion necessary for amplification. A recommended solution to circumvent this problem was the use of four-level emission schemes, which decouples the terminal laser level from the ground state from which the pump absorption takes place. Unfortunately, the existing data on optical spectra of such systems was quite scarce and selection of a suitable system was not easy. Contrary to the envisaged advantages of the four-level scheme, the first optical maser was based on a diluted ruby crystal operating in a three-level scheme; the success was based on existence of ruby crystals of quite good quality, used already for construction of masers, on the existence of strong Xe gas discharge lamps, well absorbed by the Cr^{3+} ion in ruby, and on re-evaluation of the quantum efficiency of ruby that indicated a value considerably larger than inferred from the previous studies. Demonstration of a four-level system was hampered by lack of spectroscopic data; however, very soon after the experiment with ruby, pure four-level infrared (~ 2.6 μm) laser emission was reported at low temperatures in the CaF_2 crystal doped with U^{3+}. A new name was found for these devices and processes, LASER, meaning Light Amplification by Stimulated Emission of Radiation. These successes stimulated an explosive investigation of the doped crystals for identification of new active materials (new crystals, new laser active ions), for improved theory and design of the optical resonators and for higher-performance pumping systems. Very soon the classes of active materials were extended to include atomic or molecular gases, organic or inorganic liquid solutions,

semiconductors, defects in crystals (color centers), other types of transparent materials (glasses, ceramics) doped with transition ions. The high energy of the laser beam made possible observation and use of nonlinear optical processes to modify the frequency of emission. This extended permanently the possibilities of control of performances and characteristics (wavelength, temporal regime of emission) of the emitted radiation beam. Although at the time of the advent of the laser no definite application was foreseen, soon it was realized that owing to the high coherence, the laser beam could be a very important carrier of energy and information. This determined an ever expanding field of applications in various fields such as information technology (information transmission, processing and display), processing of materials, materials technology, photochemistry, biology, medicine, defense, remote sensing and so on. It became also apparent that extension and optimization of the applications of laser radiation necessitates specialized lasers, with properties adapted to the need of an optimal utilization, by a more tight control of its properties (wavelength, temporal regime, power range). Owing to the quantum nature of the processes, this necessitates the extension of basic research on the quantum physics of the laser materials and of their interaction with radiation. The stimulus from applications is supplemented by the natural trend of progress in the basic research for new processes and active materials. The scale of interest became very large, from lasers of tremendously high power necessary for driving thermonuclear reactions, to lasers at the extremely low dimensional scale, nanosystems or even single-atom lasers. Obviously, covering this scale necessitates a broad field of approaches that encompass a large variety of processes and active materials. Thus the laser became one of the most important scientific and technological achievements of the 20th century. Combining these processes with the control of optical properties (propagation, control of emission, nonlinear properties) of materials, a new branch of science, photonics, concerned with generation of photons with controlled properties and their use emerged. This paper discusses some actual problems and prospect for future research in quantum electronics in optical range in materials activated with ions from transitions groups, especially rare earths. The research performed in this direction at the Laboratory of Solid-State Quantum Electronics Laboratory from the National Institute for Laser, Plasma and Radiation Physics Bucharest will be also mentioned.

2. ACTIVE MATERIALS FOR QUANTUM ELECTRONICS

2.1. TYPES OF DOPED ACTIVE MATERIALS

The doped active materials for quantum electronics in the optical range consist of highly transparent dielectric solids in which part of the host cations are

substituted by ions of elements from transitions groups of the Periodic Table (mainly 3d elements, rare earths or actinides) [1, 2]. The ground electronic configurations of the elements of transition groups are characterised by incomplete inner electronic shells (electronic shell 3d for the 3d elements, 4f for rare earths and 5f for actinides) whose energy levels could favour absorption or emission in the optical range. When introduced in solids, these elements ionise and loss mainly outer electrons; however, they keep electrons in the incomplete inner shells. The large number of these elements and the variety of electronic energy levels structures would, in principle, enable a large base of selection of laser active ions for the desired range of laser emission processes. Hosts for these ions can be bulk materials (single crystals, glasses, transparent ceramics), materials with restricted geometries (thin films, fibres), nanomaterials (nanocrystals), composites glass-ceramics, doped band-gap photonic crystals or fibers. The role of the host material is to confine desired concentrations of active ions in similar structural centers that grant the necessary absorption and emission properties. Usually in case of doped systems, hosts with cations of size and valence state similar to those of the doping ion are chosen; this is not always possible in case of some hosts with interesting properties, such as a certain local structure and symmetry of the cationic sites, hosts of very high thermal conductivity and so on. When the valence state is different from that of the host cation the overall electric balance of the crystal can be restored by ionic vacancies or by special means, such as co-doping with a different cationic species in a different valence state, which usually substitutes another type of cationic site of the host material.

In these laser materials the active ion interacts statically or dynamically with the constituents of the lattice and these interactions could modify the quantum state (the energy levels, the optical transition properties) as well as the dynamics of de-excitation of the ion. The static interactions depend strongly on the distance between the ion and these constituents of the host lattice, and usually the interactions with the closest neighbours are dominant. Thus a structural center can be defined as the active ion together with the whole ensemble of neighbours that determine or influence sizably the essential features of the quantum state of this ion; usually this ensemble includes the nearest anionic and, sometimes, also the nearest cationic sites.

The most used laser materials are bulk materials such as single crystals, glasses or transparent ceramics, although materials with restricted geometries such as fibres or thin films have already e well defined position. Recently, interest was risen by nanosystems such as nanocrystalline powders and ceramics, composites glass-nanocrystallites, doped photonic crystals and so on; although in case of the dielectric host materials size-confinement effects such as those connected with the forbidden gap in semiconductor quantum dots are not expected to play important role, other size-dependent effects, such as the electron-phonon or energy transfer processes could show interesting particularities of scientific or applied interest.

The single crystals are the most suitable hosts for the laser active ions. The crystals can be produced by different techniques, crystallization from melt or from flux solution, the first method being usually the most productive and giving high quality crystals. Indeed, the most important laser crystals, such as the garnets, vanadates, sesquioxides, and so on are usually produced by the Czochralski method (pulling from melt). A major problem with production of the oxide laser crystals is the high melting point and the difficult conditions of crystallization; these techniques are expensive, the compositional versatility is low, the technological yield is reduced. Generally, bulk crystalline hosts that offer for substitution a unique cationic site are selected in order to grant identical active centers. Although due to size differences from the host cation the doping ion could distort the local structure and symmetry of the occupied crystallographic site, when the centers are well isolated (low doping concentrations, no structural defects) all them will be practically identical. However, perturbations of the structure could occur owing to the disordering of the near cationic coordination spheres caused by the statistics of distribution of the active (and of the charge-compensating ions) at the available crystallographic sites. Usually the distribution of the doping ions in crystals is random and the probability of occupation of each of the available sites is the same; in this case, statistical ensembles of doping ions in near lattice sites can occur even at very low concentrations. In case of the charge-compensated crystals the distribution of the ions that accomplish the compensation could be correlated with that of the doping laser ions, the degree of correlation depending on the structure of the material and on the thermodynamic conditions offered by the production technology. In special situations clustering of the doping ions could take place. The disordering of the structure of active centers could also occur in crystals with multiple occupancy of a given cationic site. Due to the discrete structure of the crystalline lattice, a variety of perturbed structural centers could occur owing to these effects in each doped crystal.

In case of glasses there is not a well defined structure for the active centers, since the number of anionic or cationic neighbours, the distances to these neighbours and the angles of bonds could differ in certain limits: thus an almost continuous distribution of slightly different structural centers could be defined. Usually these centers are occupied at random by the doping ions, although preference for some sites could sometimes occur. At the other extreme of size-scale there are the nanocrystalline laser materials with sizes from tens to hundreds of nm. These materials can be produced by different techniques such as co-precipitation or sol-gel production of a precursor, followed by calcination, direct combustion and so on and the sizes of the nanocrystallites can be controlled by thermal treatment. Intermediate on size-scale are the transparent crystalline ceramics that emerged recently [3–5] as promising substitutes for crystals, especially for cases where the anisotropy of physical properties does not exist (cubic crystals) or can be neglected. Since the ceramic techniques enable production of transparent bodies at

temperatures around 70% from melting temperature, they are especially promising for refractory materials such as oxides. The transparent ceramics consist of crystallite grains of different orientations, and showing a very high degree of compaction. The ceramic oxide materials can be produced by two basically different methods: (i) the solid-state mixing of oxides and synthesis of the doped material followed by high pressure isostatic compression and vacuum sintering; (ii) precipitation from solution of doped nanocrystalline material, followed by vacuum sintering. The sizes of the grains in these ceramics and the degree of compaction is determined by the technological process: in case of ceramics produced from nanocrystalline material if the size of grains is kept low (hundreds of nm to microns) the transparency of ceramic is quite poor since a high volume of pores between the ceramic grains, that diffuse the light, is present. The ceramics become fully transparent when the sizes of grains are of the order of tens of microns; this determines a very tight compaction and the density of pores becomes very small, under 1 ppm. The ceramics techniques offer several important advantages over crystal growth, especially for materials of high melting point: higher technological yield, much lower cost, and ability to produce very large components. Moreover, the ceramics show an enhanced compositional versatility: transparent bodies of materials that do not melt congruently or doping concentrations much higher than for crystals can be obtained and the composition or doping is homogeneous over the entire ceramic body. An interesting class of materials is that of glass-ceramic composites, in which nanocrystallites of a component of glass are precipitated by thermal treatment. By a suitable selection of the materials and conditions of precipitation, nanocrystallites with properties more suitable for laser emission than the whole glass and which incorporate almost all the laser ions are obtained, and these can be surrounded by a glass body with some properties such as thermal conductivity, superior to the crystallites. Typical examples are the composites consisting of rare earth doped fluoride crystals precipitated in oxide glasses.

In all these materials besides the normal structural centers, determined by the structure of the host material, defective centers could be formed at or near surface, since the neighbouring anionic and cationic coordination spheres are incomplete. The ratio of these two types of centers depends on size: in the nanocrystalline materials and nanoceramics, where the ratio of surface to volume is large, the proportion of defective centers could be very high; by contrary, in transparent ceramics with grains of tens of microns, the proportion of surface centers is already very small and can be safely neglected; this is so much in case of bulk crystals or glasses.

2.2. STATIC INTERACTIONS

The static interactions between the doping ions and their neighbours in the laser materials could influence the energy level structure and the probabilities of

the optical transitions. The main static effects of the host material on the positions of the energy levels of the doping ions are:

A. Modification of the distribution (expansion) of the electronic cloud of the doping ions due especially to the covalence of the bonds with the ligands, leading to the reduction of the electron-electron interaction. This effect is known as the *nephelauxetic* ("*cloud expansion*" in Greek) *effect.*

B. The crystal field interaction that accounts for the symmetry-dependent effects of the presence of the charged constituents of the lattice around the considered laser ion.

Due to these effects, the Hamiltonian that describes the state of the laser ion in a transparent host can be written

$$H = H_0' + H_{cr} \tag{1}$$

where H_0' is a free ion-like Hamiltonian whose parameters, especially the Racah $E^{(1)}$ and $E^{(3)}$ parameters are modified by the nephelauxetic effect and H_{cr} is the crystal field Hamiltonian.

Modification of the Racah parameters by the nephelauxetic effect in solids reduces the energies of the electronic configurations, of the spectral terms and of barycentre of the electronic manifolds of the doping ion compared with the free ions. The nephelauxetic effect is determined essentially by the nature of the laser ion and of its nearest anionic coordination sphere. This in turn is determined by the composition and structure of the host crystal by: (i) the nature of ligand: the ligands can be ordered in a "nephelauxetic series" $F^- < O^{2-} < H_2O < Cl^- < Br^- < I^-$; (ii) the anionic coordination number; (iii) geometry of the first anionic coordination sphere; (iv) nearest cation-anion distances; (v) presence in the composition of host of other types of cations that share the oxygens with the laser ion can reduce the nephelauxetic effect.

The crystal field interaction is determined mainly by the nearest anionic coordination sphere, but the effect of farther spheres could be important in definite situations. The crystal field interaction depends on the nature of the laser ion and on the composition and structure of the crystal (nature of ligands and their valence state, number of ligands on the nearest coordination sphere, cation-anion distances, the geometrical configuration and the local symmetry of the site occupied by the laser ion). In case of the 3-d ions this interaction is stronger than the spin-orbit coupling and it can be considered as a perturbation on the states of the energy spectral terms ^{2S+1}L of the free-ion, while in case of the rare earth ions it is weaker than the spin orbit coupling and it can be considered as perturbation on the energy manifold $^{2S+1}L_J$ states. In each case this interaction raises totally or partially the residual degeneracy of the states on which it acts (Stark splitting of the energy levels). The interaction with the crystal field can be described with a Hamiltonian parametrized according to the symmetry of the interaction,

$$H_{cr} = \sum_{k,q} B_k^q O_k^q \,, \tag{2}$$

where the parameters B_k^q describe the intensity of interaction and O_k^q are tensor operators in the components L_i ($i = x, y, z$) in case of d-electron elements and in J_i components in case of rare earths. The index k is determined by the nature of the electrons: when only crystal field effects inside a given electronic configurations are considered, k takes only even values, *i.e.* $k = 2, 4$ in case of d-elements and $k = 2, 4, 6$ in case of rare earths). The index q can take any odd or even value from 0 to k, function on the local symmetry of the crystal field potential. The crystal field parameters are influenced in different degree by the various coordination spheres: while the terms with large k (6 or 4) are determined mainly by the nearest anionic sphere, the terms with low k (2 and to a much lesser extent 4) could be also influenced by farther spheres, including the nearest cationic coordination spheres. Generally the local symmetry of the crystal field interaction is similar to the local symmetry of the center, *i.e.* the symmetry of the first anionic coordination sphere, but in many instances the effects of the farter spheres could modify this symmetry. Moreover, the crystal field interaction of centers with defect structure, including those with defects in the nearest cationic sites can be different from the normal centers. The perturbation of the crystal field in the defect structures could be produced by size or electric charge differences. In this respect the crystal field interaction could be more informative than the nephelauxetic effect since it could reveal effects induced by defective structure of the farter coordination spheres.

Since the optical transitions in case of the laser ions in crystals take place between the crystal field levels, whose energy is determined by the barycentre of the electronic manifolds and by the crystal field splitting, the optical spectra will reflect the common effect of the crystal field interaction and of the nephelauxetic effect. This has two very important consequences: (i) the properties of each doped laser material will be different from other materials, offering a very large base of selection; (ii) the spectroscopic properties of the various structural centers in a given laser material will be different. These effects will manifest selectively in different optical transitions: when the shift in energy of the various structural centers is larger than the widths of the spectral lines the high-resolution optical spectrum will contain different lines for the various structural centers, while in case of low shift only an inhomogeneous broadening of optical transitions takes place.

The static interactions influence also the optical transition properties. The optical transitions of various electric multipolarity (dipole, quadrupole) or the magnetic-dipole transitions are governed by selection rules determined by parity or by electronic spin. Thus, in case of rare earth ions in crystals, these selection rules would forbid electric dipole transitions between states originating from the same electronic configuration, including the ground configuration $4f^n$. However, such

transitions are observed and they have been explained by mixtures with states from electronic configurations of opposite parity, induced by the terms of odd k of the crystal field Hamiltonian (2). Theoretical treatment of this effect, by neglecting the actual crystal field splitting of the states of the ground $4f^n$ configurations shows that the intensities of the various optical transitions inside the ground configurations can be described to a fairly good approximation by three parameters, Ω_i, with $i = 2$, 4 and 6. These parameters enable then the calculation of the Einstein coefficients, of the radiative lifetime of the emitting levels $\tau_{rad} = 1 \Big/ \sum_i A_i$ and the branching ratios $\beta_i = A_i \Big/ \sum_i A_i$ for the various emission transitions i originating from a given excited level. Generally, in case of slightly different structural centers in a given crystal the transition probabilities will be similar and thus the relative intensities of the lines could be taken as a measure of the relative concentrations of these centers. Marked departures from this rule could be observed in case of the non-Kramers rare earth ions (ions with even number of electrons in the 4f shell) for transitions that in the main (non-perturbed) center are forbidden but could be allowed for the lower symmetry perturbed centers.

A special situation holds for the strongly defective centers at or near surfaces. Since in these cases the nearest anionic environment could be strongly different from the bulk centers, the spectroscopic properties of these two categories of centers could be strongly different. This is important in case of nanomaterials, since the large proportion of surface centers could induce large differences from the bulk single crystals. Another important difference between nanomaterials and bulk materials is the modification of the radiative lifetime. Measurements on rare earth doped nanomaterials indicate that the radiative lifetime could be significantly longer than for bulk materials and this also depends on the refractive index of the medium that surrounds the nanocrystals. Thus, by immersing nanocrystalline powders in liquids of different index of refraction, an effective index of refraction can be defined, function of the individual indices of the material and liquid and on the filling factor. The radiative lifetime of the immersed nanomaterial will be inversely proportional to this effective lifetime: by choosing immersion materials with index of refraction lower than that of the bulk material of the nanocrystal, an enhancement of the radiative lifetime would be obtained. This process could be of perspective for quantum electronic devices.

2.3. DYNAMIC INTERACTIONS

The doping ions in solids also interact with the vibrations of lattice. The main effects of this interaction are: (i) non-radiative de-excitation of the excited levels, according to the gap law; (ii) broadening of the spectral lines; (iii) phonon satellites of the optical lines; (iv) splitting of the spectral lines caused in case of resonance

between the crystal field splitting and the phonon energies. These effects depend on the phonon densities of states. It was recently discussed that in case of low dimensional materials such as nanocrystals the Debye approximation for the continuous phonon density of states is no longer valid, the vibrational modes become discrete and no phonon mode exists below a certain cut-off energy [6]. This could influence the non-radiative electron-phonon relaxation between states with low energy gap, with strong influence on thermalization processes between the energy levels, leading to intense hot-band lines in conditions where such lines would be absent in bulk crystals. It is thus obvious that although quantum confinement is not expected to have strong effects in case of dielectric materials, the modified electron-phonon interaction due to the alteration of the phonon density of states could influence strongly the flow of excitation between the energy levels and the optical spectra of the doped nanocrystals.

2.4. ENERGY TRANSFER PROCESSES

The energy transfer processes induced by the static interactions (multipolar and/or exchange) between the doping ions influence strongly the flow of excitation between the energy levels of the laser materials [7, 8]. In such processes part of the energy of an ion excited by pumping (donor) can be transferred to another ion (acceptor). The flow of energy depends on the initial energy states of the donor and acceptor ions and on their energy level diagrams. Thus the absorbed energy can be down-converted, when the final states of the donor and acceptor ions are lower in energy than the initial state of the donor, or upconverted, when the final state of the acceptor ions is higher than the initial state of the donor. When both types of processes are permitted by the energy level diagram, the balance will be determined by the density of ions in excited state. The subsequent de-excitation of the final states of donor or acceptor is determined by the balance between the radiative and non-radiative (electron-phonon interaction) processes from these states. The energy transfer could have multiple relevance for the laser emission: (i) they could contribute to the non-radiative de-excitation of the levels involved in laser emission by interactions inside the system of doping ions (self-quenching of emission) or by transfer to accidental impurity ions; (ii) they enable sensitisation of emission by transfer of energy from a doping ion with good absorption (sensitizer) to another species of doping ion with good emission properties (activator).

The energy transfer processes could be static, when the excitation absorbed by donor is directly transferred to the acceptor or dynamic, when a migration of excitation over the excited level of the donor ions takes place prior to the transfer to the acceptor. The energy transfer is characterised by transfer rates that show specific dependences on the distances between the ions involved in transfer: in case of the multipolar interactions these rates are $W_{DA}^{(s)} = C_{DA}^{(s)} / R_{DA}^{(s)}$, where s takes the

values 6, 8 and 10 for dipole-dipole (d-d), dipole-quadrupole (d-q) and quadrupole-quadrupole (q-q) interaction, respectively and the microparameter $C_{DA}^{(s)}$ depends on the superposition integral between the emission spectrum of donor and the absorption spectrum of acceptor. The multipolar interactions are governed by selection rules, thus the quadrupolar contribution is absent for transitions with $|\mathrm{J}-\mathrm{J}'|>2$. In case of exchange interaction the rate is $W_{DA}^{(ex)} = (1/\tau_D)\exp\left[\gamma(1-R_{DA}/R_0)\right]$, with $\gamma = 2R_0L^{-1}$, L and R_0 being the penetration depth and the effective Bohr radius, respectively.

The energy transfer processes can be investigated from their effect on the dynamics of populations after a short excitation pulse by registering the emission decay of the donor and/or acceptor. In real systems each donor is surrounded by a particular configuration of acceptors and the response of the whole system of donors is given by the sum of contributions from the individual donors to emission. In case of bulk materials, owing to the enormous number of donors with similar properties and to the fact that the exact acceptor configurations around each donor are not known, this summation can be replaced by an averaging of the donor response over all the possible acceptor configurations. The global emission decay can be then written

$$I(t) = I_0 \exp\left(-\frac{t}{\tau_D}\right)\exp\left[-P(t)\right] \tag{3}$$

where $P(t)$ is the transfer function and $\exp[-P(t)]$ represents the acceptor ensemble-averaged survival probability of the donor in the excited state in presence of all the acceptors and τ_D is the lifetime of the donor ions in absence of energy transfer.

The process of averaging depends on the model of acceptor ions distribution in the crystal. Thus by assuming a uniform continuous distribution of acceptors with a constant density at each geometrical point of space, in case of an individual multipolar interaction s the transfer function becomes [9]

$$P(t) = \frac{4}{3}\pi n_A \Gamma\left(1-\frac{3}{s}\right) C_{DA}^{3/s} t^{3/s} \tag{4}$$

where $\Gamma(x)$ is the Euler function. With this approximation the multipolarity s can be simply determined from the fit of theory with the experimental emission decay. However, Eq. (4) fails to describe accurately the beginning of decay since, owing to the finite acceptor density at the donor site, the slope of $P(t)$ at $t = 0$ becomes infinite. Moreover, Eq. (4) is restricted to a unique type of multipolar interaction. These shortcomings can be removed by assuming a discrete distribution of the acceptors [10, 11]. In case of a random and equiprobable occupancy of the available sites by acceptors and assuming a unique type of acceptors the transfer function is given by

$$P(t) = -\sum_{i=1}^{N} \ln\left[\left(1 - C_A\right) + C_A \exp\left(-W_i t\right)\right], \tag{5}$$

with summation extended over all the lattice sites available to acceptors. Thus the transfer function $P(t)$ can be determined simply if the individual transfer rates W_i to the acceptor placed ions is known. Eq. (3) with function $P(t)$ given by Eq. (5) describes correctly the evolution of emission over all the temporal range. It can also be used in complex situations such as mixed interactions between donor and acceptor.

Eq. (5) shows a complex dependence of emission on the acceptor relative concentration C_A and on time. However, for long times after the exciting pulse, Eq. (5) can be approximated by the compact equation (4) (the disordered regime of static transfer) while at early time a quasi-linear dependence on time is obtained (ordered regime), $P(t) = C_A \sum_i W_i^{cr} t$. At high donor concentrations the migration of excitation over the donor level prior to transfer to acceptors could take place. This induces an additional exponential modulation of emission intensity [12], $\exp(-\bar{W}t)$ in Eq. (3). The effect of this term is usually observed at long times after beginning of decay.

With the transfer function $P(t)$ the rate equation for the population of the excited state of the donor after a short pulse excitation can be written

$$\frac{\mathrm{d}n_D}{\mathrm{d}t} = -\frac{n_D}{\tau_D} - \frac{\mathrm{d}P(t)}{\mathrm{d}t} n_D \tag{6}$$

while that of the acceptor is

$$\frac{\mathrm{d}n_A}{\mathrm{d}t} = -\frac{n_A}{\tau_A} + \frac{\mathrm{d}P_{DA}(t)}{\mathrm{d}t} n_D - \frac{\mathrm{d}P_{AA}(t)}{\mathrm{d}t} n_A \tag{7}$$

where the function $P_{AA}(t)$ accounts the possible energy transfer processes inside the system of acceptor ion after the transfer from donor. The solution of Eq. (6) is non-exponential in time, while that of Eq. (7) is a complex evolution with rise of emission, followed by decay. The discussion above refers to the case when the whole emission of donor or acceptor ions is recorded. However, as discussed in Section 2.2, the presence of doping ions in near lattice sites could produce resolvable spectral effects manifested in apparition of spectral satellites. When energy transfer could take pace between these ions, the decay functions for each spectral satellites would be different, owing to the differences between the distributions of acceptors around donor in case of each type of perturbed centers.

In the case of the doped nanocrystals the problem of energy transfer is more complex because of the presence of a large proportion of defective surface centers.

Thus, both the system of donor ions and that of acceptor cannot be considered as homogeneous and the distribution of acceptors around the various donors differs in very large limits.

3. HIGH RESOLUTION SPECTROSCOPY AND EMISSION DYNAMICS

3.1. SPECTROSCOPIC PROPERTIES OF DOPED CRYSTALS

As discussed above, the distribution of the doping ions and of the charge compensating ions in the crystalline lattice of the host materials can create a large variety of structural centers. These centers show in the optical spectra of the laser materials as satellites of the lines corresponding to the main (unperturbed, isolated ion) center. Some typical examples of such structures are:

3.1.1. Multicenter structure in case of rare earth doped garnet crystals

The garnets have a cubic crystalline structure with eight chemical units $A_3B_2C_3O_{12}$. There are three structural cationic sites, the ions A are surrounded by a distorted dodecahedron of eight O^{2-} ions (c-sites, of D_2 local symmetry), the ions B are surrounded by a trigonally-distorted octahedron of O^{2-} ions (a-sites of C_{3i} symmetry), while the ions C are surrounded by an O^{2-} tetrahedron (d-sites of S_4 symmetry). In case of yttrium aluminium garnet $Y_3Al_5O_{12}$ (YAG), $A \equiv Y^{3+}$, while $B = C \equiv Al^{3+}$. However, the high-temperature (melt-grown) garnets have usually an excess of A species, that can substitute part of the octahedral sites occupied normally by the B ions (A antisites). None or very small concentrations of antisites occur in the low-temperature YAG crystals, such as those grown from flux [13–15].

The rare earth doped YAG is a typical example of laser material where additional charge compensation is not necessary. The optical spectroscopy indicates that the overwhelming part of the RE^{3+} ions doped in the garnet crystals enter in the dodecahedral sites c, although a very small fraction of such ions in octahedral sites was detected, for instance, in case of Er^{3+} or Nd^{3+} in YAG. At the same time, the transition d-elements enter in octahedral or/and tetrahedral sites.

In case of random placement of the doping ions or of defects in the crystalline lattice, the probabilities of occurrence for the various associations of the active ion with n of these ions or defects placed on a coordination sphere with m sites is

$$P_{nm} = \frac{m!}{n!(m-n)!} C^n (1-C)^{m-n} \tag{8}$$

This equation can be used for identification of the nature of the spectral satellites and for testing the validity of various structural and placement distribution

models. In case of YAG a large variety of optical satellites was put into evidence by high-resolution studies at low temperatures: (i) Satellites P_i induced by perturbing antisites Y^{3+} (a) at the c-site of the RE^{3+} ions (Nd^{3+}, Er^{3+}, Pr^{3+}, Tm^{3+}, etc.) [16–20]; (ii) Satellites induced by antisites Y^{3+} (a) at the a-site occupied by Cr^{3+} [21]; (iii) Satellites M_i induced by RE^{3+} ion pairs: in case of Nd^{3+} in YAG, satellites due to pairs of first M_1- or second M_2 are observed in most of the optical transitions [17–19]; (iv) Satellites induced at the c-site by sensitizers from octahedral (Cr^{3+}), tetrahedral (Fe^{3+}) or dodecahedral sites [22]. For all these satellites (cases (i) to (iv)) the relative intensities of the satellites and of the line N corresponding to isolated RE^{3+} centers are well described by the statistics of equiprobable random placement, Eq. (9). No satellite attributable to perturbations caused by anionic impurities, such as OH^- in the vicinity of RE^{3+} ions was clearly identified.

The discrete chain of crystal filed perturbations inside of these associations and the presence of optical satellites show that the systems of dopant ions are not homogeneous but they are rather inhomogeneous systems composed of homogeneous subsystems. For the subsystems connected with associations of active ions or with sensitizers, this particularity is further enhanced by a selective manifestation of the energy transfer processes.

3.1.2. Trivalent rare earth doped strontium hexaaluminate

Hexagonal Strontium hexaaluminate doped with Nd^{3+} was investigated recently as host for short-wavelength laser emission on transition $^4F_{3/2} \rightarrow {}^4I_{9/2}$, owing to its structure that favours weak nephelauxetic effect and moderate crystal field interaction [23]. In this crystal Nd^{3+} substitutes Sr^{2+} ions in (2d) sites of D_{3h} symmetry, placed on the mirror plane of the crystal, that connects two spinel-like structures of Al^{3+} complexes. The cation in the (2d) site is surrounded by $12O^{2-}$ ions; each such site has six (2d) nearest neighbour (2d) sites placed on the mirror plane. Co-doping with Mg^{2+}, which substitutes part of Al^{3+} ions, was necessary in order to preserve the electric neutrality. Moreover, it was found that adding La^{3+} (and an additional amount of Mg^{2+}) facilitates the congruent melting and crystal growth by Czochralski technique and thus the chemical composition becomes $Sr_{1-x}Nd_yLa_{x-y}Mg_xAl_{12-x}O_{19}$ (Nd:ASL). The high-resolution spectroscopy of this crystal function on the composition parameters x and y indicates [24] the presence of two families of structural centers, C_1 and C_2, the relative concentration of the first being described by a law $1-(1-x)^6$ and that of the second, by $(1-x)^6$. According to Eq. (7) these dependences correspond to a structural model in which the C_2 centers are Nd^{3+} ions for which all the six n.n. (2d) sites are occupied only by Sr^{2+} ions, while in case of C_1 centers one up to all six of these sites are occupied at random by trivalent Nd^{3+} or La^{3+} ions. The energy levels of these two centers

differ, especially for the excited manifold $^4F_{3/2}$, and thus both the absorption and emission properties are different. The concentration dependence of the occurrence probability, together with arguments concerning the crystal growth indicate that most suitable for laser emission are the ASL crystals with large (≥ 0.4) x parameters.

3.1.3. Trivalent ion doping of calcium fluoride

Calcium fluoride is an interesting laser material since it can accommodate a large variety of trivalent rare earth and actinide ions. This crystal has cubic symmetry, the Ca^{2+} ion is placed at the centre of a cube of eight F^- ions and each the second cube is empty in order to preserve the charge neutrality. Doping with trivalent ions requires charge compensation and this can be accomplished by excess F^- ions that could enter in the empty cubes near the trivalent ion leading to a variety of perturbed centers; moreover, this compensation is quite unstable and difficult to control. It was then found that a stable and controllable solution could be co-doping with monovalent ions. The Electron Paramagnetic Resonance investigation of CaF_2 crystals doped with U^{3+} and compensated with monovalent ions(Li^+, Na^+, K^+, Ag^+) revealed [25–27] the presence of a variety of centers of different symmetries, in correlation with the possibilities of placement of the charge-compensating ions in vicinity of U^{3+}.

3.2. EMISSION DYNAMICS IN LASER MATERIALS

3.2.1. Emission decay and quantum efficiency of Nd-doped laser materials

Early measurements of emission decay after a short pulse excitation of low intensity in Nd:YAG with the usual 1 at.% Nd concentration have been interpreted in a model of exponential decay. However, subsequent measurements at various Nd concentrations C_{Nd} evidenced [28–31] a complex non-exponential evolution in time, dependent on C_{Nd}. Such behaviour was observed subsequently in many Nd-doped laser materials. This indicates the presence of energy transfer inside the system of Nd^{3+} ions. According to the energy level diagram, the transfer is accomplished by cross-relaxation between a Nd ion excited on the emitting level $^4F_{3/2}$ and a Nd ion in its ground state: $(^4F_{3/2}, {}^4I_{9/2}) \rightarrow (^4I_{11/2}, {}^4I_{11/2})$. In case of the oxide crystals this cross-relaxation is followed by efficient electron-phonon de-excitation of level $^4I_{15/2}$, thus all the excitation involved in this process is lost as heat and the characteristics of the energy transfer can be inferred only from the emission of donor. In many laser materials the ion-ion interaction responsible for cross-relaxation contains exchange (leading to a fast drop of emission at the beginning of decay, with an extent which indicates that this interaction is important only for the nearest neighbours Nd ions) and dipole-dipole interaction, $W_i = W_i^{ex} +$

+ W_i^{d-d}, while for other crystals only the last interaction is apparently active. The limitation of the multipolar interactions to the dipole-dipole interaction is consistent with the selection rules for the transitions involved in the down-conversion cross-relaxation. With increasing C_{Nd}, the decay evidences the onset of migration over the donor level prior to transfer to acceptors for all three materials. When migration is caused by dipole-dipole interaction between donors, the migration-assisted transfer rate depends quadratically on C_{Nd}, $\overline{W} = \overline{W}_0 C_{Nd}^2$.

Since the transfer function $P(t)$ has a sub-linear dependence of time, while the migration-assisted term has a linear dependence, the relative importance of these two transfer processes changes in time: the direct transfer, which imposes a non-exponential character of decay dominates the beginning of decay, while the effect of the migration, which induces an exponential behaviour, becomes more evident at long times. The border between these two parts of decay is not sharp; moreover, owing to a different C_{Nd}-dependence of the function $P(t)$, almost linear in C_{Nd}, especially at low concentrations, and of the migration-assisted process (quadratic in C_{Nd}), this border moves toward shorter times with increasing concentration. Thus the Nd concentration not only accelerates the decay, but changes also its shape. It is thus evident that an exponential approximation at different Nd concentrations using the same interval of time for calculation of the time necessary for an e-drop of emission introduces systematic errors in calculation of emission quantum efficiency. The experimental microparameters of the interactions that determine the energy transfer at low pump intensities for several important laser materials are given in Table 1.

Table 1

Measured energy transfer parameters for several Nd-doped laser materials

Laser material	W_1 10^6 s^{-1}	C_{DA} 10^{-40} $cm^6 s^{-1}$	$\overline{W}$ s^{-1} (at.% Nd)^2	Comments
Nd:YAG	2.5	1.8	240	Up to 9 at.% Nd
Nd:Y_2O_3	4.0	37	450	Up to 4-5 at.% Nd
Nd:$GdVO_4$		3.6	2050	Presence of the superexchange interaction Uncertain

The emission decay law (3) enables the calculation of the effect of various non-radiative processes on the emission quantum efficiency

$$\eta_{qe} = \frac{1}{\tau_D} \int_0^\infty \frac{I(t)}{I(0)} \mathrm{d}t \tag{9}$$

At low C_{Nd}, when the energy transfer processes can be neglected, the intrinsic quantum efficiency, influenced only by the electron-phonon interaction is given by

the ratio of the measured luminescence lifetime to the calculated radiative lifetime

$$\eta_{qe}^{(i)} = \frac{\tau_D}{\tau_{rad}} = \frac{1}{1 + W_{nr}\tau_{rad}}. \tag{10}$$

In case of Nd:YAG, $\eta_{qe}^{(i)} \sim 0.99$, *i.e.*, very close to unity. With the decay law (4) in presence of static and migration-assisted energy transfer, the extrinsic emission quantum efficiency is

$$\eta_{qe}^{(t)} = \frac{1}{\tau_D}\int_0^\infty \exp\left(-\frac{t}{\tau_D}\right)\exp[-P(t)]\exp(-\bar{W}t)\mathrm{d}t. \tag{11}$$

By using the energy transfer function (5), emission quantum efficiency becomes

$$\eta_{qe}^{(t)} = \frac{1}{1 + \bar{W}\tau_D}\exp[-b(C_{Nd})C_{Nd}] \tag{12}$$

where

$$b(C_{Nd}) = \sum_i \frac{W_i}{\tau_D^{-1} + \bar{W} + W_i} \tag{13}$$

Equation (11) enables the definition of an effective lifetime of emission,

$$\tau_{eff} = \tau_D \eta_{qe}^{(t)} = \frac{\tau_D}{1 + \bar{W}\tau_D}\exp\left(\sum_i \frac{W_i}{\tau_D^{-1} + W_i + \bar{W}} C_{Nd}\right) \tag{14}$$

These equations show that the emission quantum efficiency can be calculated if the structure of the crystalline lattice (which determines the summation in Eq. (17)) as well as the nature and characteristic parameters of the energy transfer processes are known. The calculated η_{qe} for two important Nd laser materials at different C_{Nd} is given in Table 2

Table 2

Calculated emission quantum efficiencies for various Nd concentrations in YAG and $GdVO_4$

Nd concentration, at.%	Nd:YAG	Nd:$GdVO_4$
0.5	0.88	0.88
1.0	0.80	0.73
2.0	0.58	0.45
3.0	0.41	0.28
4.0	0.30	0.18
5.0	0.23	0.13

The emission quantum efficiency can be measured either by direct methods, that measure the intensity of emission and compares it with the absorption, or by indirect methods, based on the effects of the non-radiative de-excitation. The direct methods are large errors owing to the very complex calibration procedures. Since in case of oxide laser materials all the excitation which is not used for emission is transformed into heat, indirect methods based on heating effects could be used for estimation of the emission quantum efficiency. However, these methods do not provide directly η_{qe}, but the product $\eta_q = \eta_{qe}\eta_p$ with the pump level efficiency η_p, that describes the fraction of excitation quanta absorbed in the pump energy level that populate the emitting level. In case of Nd:YAG, accurate values for η_q for different Nd concentrations have been measured by different methods such as calorimetric interferometry [32], heat generation [33] or depolarisation of a probe laser beam [34]. Generally, in case of oxide laser materials, in conditions of these measurements there is no physical reason for pump level efficiency η_p lower than 1. A comparison of the experimental values for η_q with the calculated (Eq. (11)) values for η_{qe} in case of Nd:YAG is given in Fig. 1. A very good agreement between theory and experiment is observed, suggesting that indeed $\eta_p \approx 1$. This finding is in sharp disagreement with the approach used by several authors that approximate the emission decay of Nd:YAG by an exponential and calculate the emission lifetime as the duration necessary for a (1/e) drop of intensity; such approach gives $\eta_{qe} \approx 0.9$ for 1 at.% Nd:YAG [35], much larger than the 0.8 value determined by an accurate treatment of decay (Table 1). In order to accommodate such large (0.9) value for η_{qe} with the measured (0.8) η_q, a value of ~ 0.9 was assumed for η_p; physically, this was justified [33] by the presence of a quite large proportion (~ 10%) of "dead sites" of Nd in YAG, which de-excite non-radiatively by interaction with anionic impurities of high vibrational energies, such as OH^-.

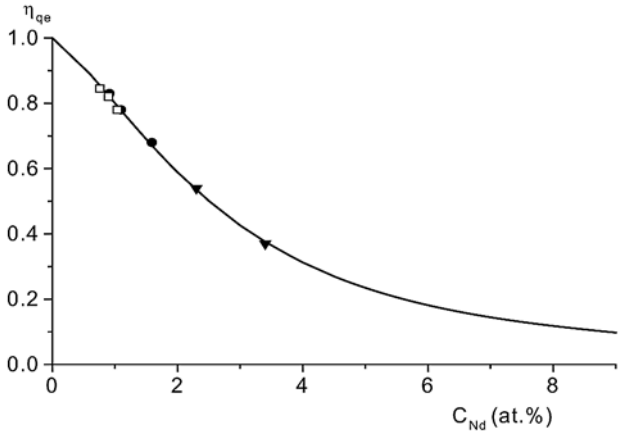

Fig. 1 – Calculated emission quantum efficiency for Nd:YAG (full line) and experimental data: emission quantum efficiency determined from heat generation (squares), calorimetric interferometry (circles), depolarisation effects (triangles).

However, the presence of such large amount of impurity OH^- in YAG could not be proved and much time and material consuming effort was wasted to eliminate such non-existing impurities. Our treatment indicates clearly that the measured quantum efficiency is exactly what can be expected due to unavoidable energy transfer processes inside the system of doping Nd ions in this material and the "dead site" hypothesis is not valid in the case of Nd:YAG.

A very interesting manifestation of the energy transfer processes is seen in case of Nd-doped strontium hexaaluminate. According to the structural models for the C_1 and C_2 centers discussed above, the distribution of the acceptors around the donor Nd ions will be different, since for center C_1 the Nd ions could substitute for any (2d) site, while for centers C_2 they cannot occupy the sites of the nearest coordination sphere of (2d) sites. Thus, the summation in Eq. (5) extends for all i sites in the case of C_1, but it is valid only for $i > 6$ in the case of C_2 center [24]. This induces a difference in decay at short times as well as a reduced emission quantum efficiency in the case of centers C_1, $\eta_{qe}(C_1) = \alpha\eta_{qe}(C_2)$; the coefficient α can be calculated by using Eqs. (12) and (13) and decreases with the Nd concentration.

3.2.2. Emission decay in sensitised laser materials

Emission decay in sensitised materials is a very powerful tool for investigation of the characteristics of energy transfer and for estimation of sensitisation efficiency. For these systems the information on the energy transfer processes inferred from the emission decay of the donor ion is supplemented by the emission decay of the acceptor ions. In cases when the perturbing effects of the ions in near lattice sites can be resolved, important selective data on transfer can be obtained from emission decay for the various spectral satellites. For instance, in the case of Cr^{3+} or Fe^{3+}-sensitized emission of Tm^{3+} in YAG, it was clearly demonstrated [22] that the energy transfer from sensitizers from the nearest coordination sphere to the Tm^{3+} ions contains contribution from superexchange and dipole-dipole coupling, while for farter sensitizers this is dominated by dipolar contribution. A similar situation was observed in the case of Nd-sensitized emission of Yb^{3+} in cubic sesquioxide Sc_2O_3 ceramics [36].

3.2.3. Energy transfer as means for depopulation of terminal laser level

Laser emission on several important optical transitions could be hampered by a lifetime of the terminal level larger than that of the emitting level. Thus, despite of very favourable emission properties, the inversion of population could be rapidly destroyed because of selfsaturation. Such case is the important transition at 3 microns $^4I_{11/2} \rightarrow {}^4I_{13/2}$ in Er^{3+} in various hosts: in case of YAG the lifetime of the terminal level is about 60 times larger than that of the emitting level and laser

emission at normal Er concentrations would not be possible. However, it was found that quite efficient is obtained at high Er concentrations. This was explained tentatively by action of upconversion process by interaction between two Er ions excited in the $^4I_{13/2}$ level, ($^4I_{13/2}$, $^4I_{13/2}$) → ($^4I_{9/2}$, $^4I_{15/2}$), followed by rapid electron-phonon de-excitation of level $^4I_{9/2}$ to the emitting level $^4I_{11/2}$. This process not only depopulates the terminal level, but reintroduces half of the population of this level back into the emitting level. The existence of such processes was indeed demonstrated [37–39] and it was shown that it can drive efficient three-micron laser emission in concentrated Er materials [40–42]; moreover, it was found that at high Er concentrations processes involving three Er ions could be active [37]. In case of low Er concentrations, energy transfer from terminal level to impurity ions could be useful.

4. DIRECTIONS OF IMPROVEMENT OF LASER PERFORMANCES

The analysis of the flow of excitation inside the laser materials indicates that actually the properties of the laser materials are not completely exploited and that important directions of development are the reduction of the quantum defect between the pump and laser quanta, the use of concentrated laser materials to improve the pump absorption efficiency, development of new laser materials such as polycrystalline ceramics, and an improved design of the laser resonator.

4.1. DIRECT PUMPING OF Nd LASER MATERIALS INTO THE EMITTING LEVEL

Although the direct pumping into the emitting level $^4F_{3/2}$ was demonstrated in the early works on diode excitation of Nd emission and in the construction of diode-pumped Nd:YAG lasers in the one-micron range [43–45], the low pump absorption at the Nd concentrations of ~ 1 at.% used traditionally in the construction of Nd:YAG lasers prevented high laser performances and it was soon replaced by the pump in the 800 nm region; the availability of stronger pump diodes in this wavelength range contributed undoubtedly to this choice. The recent advent of powerful diode lasers in a much larger range of wavelengths, together with the deeper basic knowledge and the technological progress in the field of the laser materials determines a revitalization of the direct pumping approach [46–54]. A general complication connected with the direct pumping could be the stimulated emission at the wavelength of pump; however, in case of low inversion specific to the lasers discussed here this effect can be safely neglected. It is obvious that for the directly pumped Nd lasers the pump level efficiency η_p is by definition equal to unity.

The room temperature $^4I_{9/2} \rightarrow {}^4F_{3/2}$ absorption spectra of the Nd laser materials show the existence of several transitions suitable for diode laser pumping; some of these transitions are thermally-activated (absorption hot-bands), starting from the second (Z_2), or even from the third (Z_3) Stark sublevels of the ground manifold $^4I_{9/2}$ [47–51]. These transitions use part of the thermal energy of the laser material for pumping and are more stable with respect to the changes of temperature than those originating from the lowest Stark component Z_1. Of special interest could be the laser materials for which the gap between the Stark sublevels Z_3 and Z_2 is almost coincident with that between the two Stark components R_1 and R_2 of the emitting level $^4F_{3/2}$: in this case the transitions $Z_2 \rightarrow R_1$ and $Z_3 \rightarrow R_2$ are almost degenerated and the laser diode emission spectrum could encompass the two transitions and use thus the populations of the two Stark levels Z_2 and Z_3 of the ground manifold for absorption. Such situation holds in Nd:YAG, where these two hot band transitions are separated by only 1.45 nm and show in the absorption spectrum as a two-peaked band centred on 11300 cm^{-1} (885 nm). The two peaks have nearly the same intensity at the room temperature and peak absorption coefficients of ~ 1.7 cm^{-1} for 1 at.% Nd, compared with ~ 11 cm^{-1} for the strong absorption at 809 nm into the level $^4F_{3/2}$. The FWHM of the 885 nm absorption band at the room temperature and 1 at.% Nd is ~ 2.7 nm and fits well the diode laser emission spectra, whose width is usually ~ 2 nm. Thus the effective absorption coefficient for diode pump the 885 nm band is close to the peak absorption value, while for the 809 nm band it is lower than the peak value, ~ 6 to 7 cm^{-1}, *i.e.* only by 3.5 to 4 times larger than for 885 nm. In case of Nd:YVO_4 no quasi-coincidence of two absorption bands takes place and the hot-band transitions are weak: the most favourable for direct pumping into the emitting level is the transition $Z_1 \rightarrow R_2$ at 880 nm, whose peak absorption coefficient for 1 at.% Nd is ~ 55 cm^{-1}, compared with ~ 75 cm^{-1} for the 808 nm absorption [46, 55].

Elimination of the upper quantum defect by direct pumping into the emitting level increases the quantum defect (Stokes) ratio $\eta_{qd}^{(l)} = \lambda_p / \lambda_l$ for laser emission compared with the traditional pumping into the level $^4F_{5/2}$ by 9.5% in case of the 1064 nm emission in Nd:YAG and by 8.6% in case of the 1064 nm emission in Nd:YVO_4, leading to a corresponding decrease of emission threshold and increase of the slope efficiency. Moreover, for this laser transition, the heat generation in case of efficient laser extraction is reduced by ~ 30%. In case of the 0.9 micron $^4F_{3/2} \rightarrow {}^4I_{9/2}$ laser emission a similar improvement of the laser parameters as in case of one-micron emission would be expected; however, the reduction of heat generation could be much larger, ~ 50–60%. While for some laser materials such as Nd:YVO_4 the absorption bands for direct pumping into the level $^4F_{3/2}$ at the traditional Nd concentrations of ~ 1 at.% are intense and almost complete

absorption of the pump radiation can be obtained with thin (≤ 1 mm) laser components, in other cases, such as Nd:YAG the absorption is weak; this situation could be improved by using more concentrated laser materials. Indeed, it can be shown that the effect of reduction of emission quantum efficiency on the laser threshold in case of concentrated materials can be compensated by the enhancement of pump absorption [49–51] and a significant materials-only figure of merit for the effect of Nd concentration is the product $\eta_a \eta_{qe}$. Using the calculated η_{qe} values (Table 2), it was inferred that figures of merit similar or larger than the traditional 1% Nd:YAG crystals could be obtained at quite large Nd concentrations, up to the 6–8% range. This suggests that direct pumping of concentrated Nd laser materials could improve the laser emission parameters. This was already demonstrated in recent years for some important laser materials. Some of the reported results represent the highest laser performances in absorbed power and for some cases also in input power.

4.1.1. CW Nd lasers

A. One-micron laser emission.

The 1.064 nm CW laser emission under direct pumping into the emitting level was investigated with Ti:sapphire or diode laser pumping on conventional (~ 1 at.% Nd) or concentrated Nd:YAG crystals or transparent ceramics [50–54]. Slope efficiencies in absorbed power of 0.79 under Ti:sapphire pumping and 0.75 to 0.77 under diode laser pumping are reported for conventional Nd:YAG single crystals. The direct pumping in uncoated concentrated Nd:YAG crystals (up to 3.5 at.% Nd) or ceramics (up to 6.8 at.% Nd) shows good performances. Comparison with 809 nm pumping shows that the direct 885 nm pumping increases the slope efficiency in absorbed power $\eta_{sl}^{(ab)}$ and decreases the threshold by 9 to 14%, in fairly good agreement with the expected increase of the quantum defect ratio. The ceramic Nd:YAG materials give similar performances with the single crystals of the same Nd concentration.

Similar performances are obtained with direct pumping of Nd:YVO_4: $\eta_{sl}^{(ab)}$ of 0.733 was obtained with a 0.55 at.% crystal. Laser measurements on uncoated Nd:YVO_4 crystals in a non-optimised resonator give $\eta_{sl}^{(ab)}$ of 0.70, 0.67 and 0.58 for 1, 2 and 3 at.% Nd under 880 nm pumping [56], respectively, while under 809 nm pumping this was ~ 10% lower and the emission for the 2 and 3 at.% Nd crystals could be observed only for pump powers close to threshold owing to the severe heating at this wavelength of pump. These laser data evidence again a lowering of the optical quality of the laser materials at high C_{Nd}. Recent laser emission measurements with an AR-coated 1 mm 1 at.% Nd:YVO_4 crystal under focussed Ti:sapphire pump evidence [55] a slope efficiency in incident power $\eta_{sl}^{(i)}$

of 0.8 and a total optical-to-optical efficiency of 0.79 for 1 W incident power at 880 nm, while in case of diode laser pump $\eta_{sl}^{(ab)}$ was somewhat lower, 0.75, owing to a poorer volume superposition efficiency. Very high slope efficiency was also obtained in the CW emission of directly pumped 0.5 and 1 at.% Nd:$GdVO_4$ ($\eta_{sl} = 0.8$) [57] and in the repetitively pumped 2 at.% Nd:$GdVO_4$ ($\eta_{sl} = 0.78$) [58].

B. $^4F_{3/2} \rightarrow {}^4I_{9/2}$ 0.9-micron laser emission.

The direct pumping into the emitting level transforms the quasi-three-level lasers, whose lesser emission terminates on a level close, but not coincident with the ground level, to a quasi-two-level emission. Such laser scheme is the most efficient from point of view of efficiency since the laser energy quantum is close to that of the pump radiation. Such quasi-two-level emission was reported in Nd:YAG [59, 60] and Nd:YVO_4 [46]. In case of Nd:YAG $\eta_{sl}^{(ab)}$ of 0.35 and 0.68 at pump ~ 4 times the threshold were obtained with 6 mm and respectively 3 mm long Nd:YAG crystals with 1 at.% Nd; these values exceed largely those obtained in quasi-three-level emission with 809 nm pumping. However, owing to the low absorption efficiency, the performances in input power are still modest, and a solution to overcome this situation and to reduce the deleterious effect of reabsorption would be the multi-pass end pumping. In case of a 0.7 mm 0.55 at.% Nd:YVO_4 crystal $\eta_{sl}^{(ab)}$ of 0.51 at 915 nm was obtained, compared with 0.47 for 809 nm pumping.

The Nd-doped strontium lanthanum hexaaluminate crystals with composition selected to grant high concentrations of C_1 centers give very efficient emission at 901 nm [61], owing to the weak nephelauxetic effect. Direct pumping at 866 nm demonstrated very high $\eta_{sl}^{(ab)}$, ~ 0.84, compared with 0.74 in case of the 792 nm $^4F_{5/2}$ pumping [62].

4.1.2. Repetitively Q-switched Nd lasers

The laser emission at 1064 nm of continuously pumped passively Q-switched Nd lasers under 885 nm diode laser pumping was investigated with 1 and 2.4 at% Nd:YAG crystals using Cr^{4+}:YAG saturable absorbers. In the case of the 2.4 at.% Nd crystal an average emission power of 0.95 W was obtained for 5.2 W absorbed power, an output mirror with $T = 0.05$ and absorber with initial transmission of 0.90. The repetition rate of the 37.5 ns pulses was 7.1 kHz, corresponding to pulse energy of 134 μJ and 3.6 kW peak power [63]. Changing the initial transmission of the saturable absorber and the transmission of the output mirror can modify the characteristics of emission. The obtained performances are superior to those obtained with 809 diode pumping and 1.1 at.% Nd:YAG crystal.

4.1.3. Frequency doubling of Nd laser emission

Direct pumping of the Nd lasers has a very strong effect on the overall efficiency of the nonlinear devices based on these lasers. The experiments with frequency doubling of the one-micron emission of the Nd:YAG or Nd:YVO_4 lasers shows that direct pumping into the emitting level could increase dramatically the power emitted at the second harmonic compared with the traditional pumping in the 800 nm range [64, 65]. Similar results are obtained in case of the self-frequency doubling of the Nd one-micron emission in Nd-doped nonlinear crystals such as the gadolinium oxiborate [66].

4.2. ADVANCED DESIGN OF THE LASER RESONATOR

The reduced absorption in case of direct pump of some important Nd laser materials can require non-conventional laser resonators. A solution to increase the absorption length would be the use of the edge-pumped slab concept developed in Ref. [67] for Yb lasers. In this concept the thin slab of laser material is pumped from edges by arrays of diode lasers and its size along the path of the pump radiation could be large enough to grant a good absorption; a design that enables a multiple pass of the pump beam can be used. Such approach could be particularly useful for the Nd:YAG lasers in the one-micron range with direct pumping at 885 nm.

In the case of the longitudinally pumped quasi-three-level Nd lasers with weak absorption of pump the increase of the path of laser radiation inside the laser material would enhance the reabsorption of laser emission. A solution to circumvent this shortcoming could be a laser resonator that decouples the length of absorption l' from the path of the laser beam l. This can be accomplished in multipass end-pumped resonator [68–70]; in this case $l' = nl$, where n is the number of passes. A large n could reduce drastically the thickness of the active component and decrease the reabsorption loss much below the other losses in resonator. A further reduction of thickness in order to facilitate the dissipation of heat could be achieved by using more concentrated Nd materials in the multipass concept [71].

5. CONCLUSION

The intense research on the emission properties of activated photonic materials evidences a very strong and interrelated functional relation of these properties with the composition, structure and size of the active material. The use of this relation could extend and improve the parameters of the photon sources, leading to the extension of the field of applications. Despite of the enormous

progress in the field, many scientific problems are still open and their circle is expanding. Although most researches are still performed on bulk materials or in materials with restricted geometries, recent developments indicate that very important progress could be obtained in the case of low dimensional materials, including nanomaterials.

REFERENCES

1. R. C. Powell, *Physics of Solid-State Laser Materials*, AIP Press-Springer (1998).
2. A. A. Kaminskii, *Crystalline Lasers: Physical Processes and Operating Schemes*, CRC Press Boca Raton (1996).
3. A. Ikesue, T. Kinoshita, K. Kamata, K. Yoshida, J. Amer. Ceram. Soc., 78 (1995), 1033.
4. A. Ikesue, Opt. Mat., 19 (2002), 183.
5. J. Lu, M. Prabhu, J. Song, C. Li, J. Xu, K. Ueda, A. A. Kaminskii, H. Yagi, T. Yanagitani, Appl. Phys., B 71 (2000), 469.
6. A. Tamura, Phys. Rev., B 52 (1995), 2688.
7. T. Forster, Ann. Phys., 2 (1948), 55.
8. D. L. Dexter, J. Chem. Phys., 21 (1953), 836.
9. M. Inokuti and F. Hirayama, J. Chem. Phys., 43 (1965), 1078.
10. S. I. Golubov and Yu. V. Konobeev, Sov. Phys. Solid State, 13 (1972), 2679.
11. V. P. Sakun, Sov. Phys. Solid State, 14 (1973), 1906.
12. I. A. Burnshtein, Sov. Phys. Uspekhi, 27 (1984), 579.
13. S. Geller, G. P. Espinosa, L. D. Fullman , P. B. Crandall, Mater. Res. Bull., 7 (1972), 1219.
14. C. D. Brandle and L. R. Burns, J. Cryst. Growth, 26 (1974), 169.
15. J. Chenevas, J. C. Joubert, M. Marezio, B. Fernarnd, J. Less Common Met., 62 (1978), 373.
16. Yu. K. Voronko and A. A. Sobol, Phys. Status Solidi, A27 (1975), 657.
17. V. V. Osiko, Yu. K. Voronko, A. A. Sobol, Crystals, Vol. 10, Springer-Verlag, Berlin-Heidelberg-New York (1984), p. 87.
18. A. Lupei, V. Lupei, S. Georgescu, W. M. Yen, J. Luminesc., 39 (1987), 35.
19. V. Lupei, A. Lupei, C. Tiseanu, S. Georgescu, C. Stoicescu, P. M. Nanau, Phys. Rev., B 51 (1995), 8.
20. A. Lupei, V. Lupei, E. Osiac, J. Phys.: Condens. Matter, 10 (1998), 9701.
21. V. Lupei, L. Lou, G. Boulon, A. Lupei, J. Phys.: Condens. Mat., 5 (1993), L 35.
22. V. Lupei, A. Lupei, G. Boulon, Phys. Rev., B 53 (1996), 14818.
23. G. Aka, E. Reino, D. Vivien, F. Balembois, P. Georges, B. Ferrand, Trends in Optics and Photonics, 68 (2002), 329.
24. A. Lupei, V. Lupei, L. Gheorghe, D. Vivien, G. Aka, P. Aschehoug, J. Appl. Phys., 96 (2004), 3057.
25. V. Lupei, C. Stoicescu, I. Ursu, J. Phys., C 9 (1978), L 317.
26. I. Ursu, V. Lupei, Bull. Magn. Res., 6 (1984), 162.
27. I. Ursu, V. Lupei, Magn. Res. Rev., 10 (1986), 253.
28. V. Lupei, A. Lupei, S. Georgescu, C. Ionescu, Opt. Commun., 60 (1986), 59.
29. I. Ursu, V. Lupei, A. Lupei, W. M. Yen, Rev. Roum. Phys., 32 (1987), 1003.
30. V. Lupei, A. Lupei, S. Georgescu, I. Ursu, Appl. Phys. Lett., 59 (1991), 905.
31. V. Lupei, A. Lupei, Phys. Rev., B 61 (2000), 8087.
32. K. K. Deb, R. G. Buser, J. Paul, Appl. Opt., 20 (1981), 1203.
33. T. Y. Fan, IEEE J. Quantum Electron., 29 (1993), 1457.
34. I. Shoji, Y. Sato, S. Kurimura, V. Lupei, T. Taira, A. Ikesue, K. Yoshida, Opt. Lett., 27 (2002), 234.
35. A. A. Kaminskii, *Laser Crystals*, Springer 1981.

36. V. Lupei, A. Lupei, A. Ikesue, Appl. Phys. Lett., 86 (2005), 111118.
37. V. I. Zhekov, T. M. Murina, A. M. Prokhorov, S. Georgescu, V. Lupei, I. Ursu, Sov. J. Quantum Electron., 16 (1986), 274.
38. A. Lupei, V. Lupei, S. Georgescu, I. Ursu, V. I. Zhekov, T. M. Murina, A. M. Prokhorov, Phys. Rev., B 41 (1990), 10923.
39. V. I. Zhekov, T. M. Murina, A. M. Prokhorov, M. I. Studenikin, S. Georgescu, A. Lupei, V. Lupei, I. Ursu, JETP Lett., 52 (1990), 670.
40. V. Lupei, S. Georgescu, V. Florea, IEEE J. Quantum Electron., 29 (1993), 426.
41. M. Pollnau, W. Luthy, H. P. Weber, Phys. Rev., A 49 (1994), 3309.
42. S. Pollack, M. Chang, J. Appl. Phys., 70 (1991), 7227.
43. R. Newman, J. Appl. Phys., 34 (1963), 437.
44. M. Ross, Proc. IEEE, 56 (1968), 196.
45. L. J. Rosenkrantz, J. Appl. Phys., 43 (1972), 4603.
46. T. Kellner, C. Czeranowski, G. Huber, Conf. on Novel Lasers and Devices, Munich (1999) Techn. Dig. LTUD 2-1.
47. R. Lavi, S. Jackel, M. Winik, E. Lebiush, I. Tzuk, M. Katz, I. Paiss, Appl. Opt., 38 (1999), 7382.
48. R. Lavi, S. Jackel, Appl. Opt., 39 (2000), 3093.
49. V. Lupei, A. Lupei, S. Georgescu, T. Taira, Y. Sato, A. Ikesue, Phys. Rev., B 64 (2001), 092102.
50. V. Lupei, T. Taira, A. Lupei, N. Pavel, I. Shoji, A. Ikesue, Opt. Commun., 195 (2001), 225.
51. V. Lupei, A. Lupei, N. Pavel, T. Taira, I. Shoji, A. Ikesue, Appl. Phys. Lett., 79 (2001), 590.
52. V. Lupei, A. Lupei, N. Pavel, T. Taira, A. Ikesue, Appl. Phys., B 73 (2001), 1.
53. V. Lupei, N. Pavel, T. Taira, IEEE J. Quantum Electron., 38 (2002), 240.
54. V. Lupei, A. Lupei, S. Georgescu, B. Diaconescu, T. Taira, Y. Sato, S. Kurimura, A. Ikesue, J. Opt. Soc. Am., B 19 (2002), 360.
55. Y. Sato, T. Taira, N. Pavel, V. Lupei, Appl. Phys. Lett., 82 (2003), 844.
56. V. Lupei, N. Pavel, T. Taira, Opt. Commun., 201 (2002), 431.
57. V. Lupei, N. Pavel, Y. Sato, T. Taira, Opt. Lett., 28 (2003), 2366.
58. T. Ogawa, Y. Urata, S. Wada, K. Onodera, H. Machida, H. Sagae, M. Higachi, K. Kodaira, Opt. Lett., 28 (2003), 2333.
59. V. Lupei, G. Aka, D. Vivien, Opt. Commun., 204 (2002), 399.
60. V. Lupei, N. Pavel, T. Taira, Appl. Phys. Lett., 81 (2002), 2677.
61. G. Aka, D. Vivien, V. Lupei, Appl. Phys. Lett., 85 (2004), 2685.
62. V. Lupei, G. Aka, D. Vivien (to be publ.).
63. V. Lupei, N. Pavel, T. Taira, Appl. Phys. Lett., 80 (2003), 4309.
64. V. Lupei, N. Pavel, T. Taira, Appl. Phys. Lett., 83 (2003), 2366.
65. V. Lupei, G. Aka, J. Appl. Phys., 97 (2005), 056104.
66. V. Lupei, G. Aka, D. Vivien, Appl. Phys. Lett., 81 (2002), 811.
67. T. S. Rutherford, W. M. Tullock, E. K. Gustafson, R. L. Byer, IEEE J. Quantum Electron., 36 (2000), 205.
68. T. Y. Fan, IEEE J. Quantum Electron., 28 (1992), 2692.
69. P. J. Morris, W. Luthy, H. P. Weber, Opt. Commun., 104 (1993), 97.
70. A. Giesen, H. Hugel, A. Voss, K. Wittig, U. Braud, H. Opower, Appl. Phys., B 58 (1994).
71. V. Lupei, Opt. Mat., 24 (2003), 353.